J. Cent. South Univ. (2015) 22: 1079−1086
DOI: 10.1007/s11771-015-2619-2

Springer

Impact of permafrost degradation on embankment deformation of Qinghai−Tibet Highway in permafrost regions

PENG Hui(彭惠)[1, 2, 3], MA Wei(马巍)[1], MU Yan-hu(穆彦虎)[1], JIN Long(金龙)[2]

1. State Key Laboratory of Frozen Soil Engineering, Cold and Arid Regions Environmental and Engineering Research Institute, Chinese Academy of Science, Lanzhou 730000, China;
2. Key Laboratory of Highway Construction & Technology in Permafrost Regions, Ministry of Transport, CCCC First Highway Consultants Co., Ltd., Xi'an 710065, China;
3. University of Chinese Academy of Science, Beijing 100049, China

Abstract: Based on long-term monitoring data, the relationships between permafrost degradation and embankment deformation are analyzed along the Qinghai−Tibet Highway (QTH). Due to heat absorbing effect of asphalt pavement and climate warming, permafrost beneath asphalt pavement experienced significant warming and degradation. During the monitoring period, warming amplitude of the soil at depth of 5 m under asphalt ranged from 0.21 °C at the XD1 site to 0.5 °C at the KL1 site. And at depth of 10 m, the increase amplitude of ground temperature ranged from 0.47 °C at the NA1 site to 0.07 °C at the XD1 site. Along with ground temperature increase, permafrost table beneath asphalt pavement decline considerably. Amplitude of permafrost table decline varied from 0.53 m at the KL1 site to 3.51 m at the NA1 site, with mean amplitude of 1.65 m for 8 monitoring sites during the monitoring period. Due to permafrost warming and degradation, the embankment deformation all performed as settlement at these sites. At present, those settlements still develop quickly and are expected to continue to increase in the future. The embankment deformations can be divided into homogeneous deformation and inhomogeneous deformation. Embankment longitudinal inhomogeneous deformation causes the wave deformations and has adverse effects on driving comfort and safety, while lateral inhomogeneous deformation causes longitudinal cracks and has an adverse effect on stability. Corresponding with permafrost degradation processes, embankment settlement can be divided into four stages. For QTH, embankment settlement is mainly comprised of thawing consolidation of ice-rich permafrost and creep of warming permafrost beneath permafrost table.

Key words: Qinghai−Tibet Highway (QTH); permafrost degradation; embankment deformation; thawing settlement

1 Introduction

Permafrost change is a sensitive climate warming indicator [1]. In recent decades, permafrost warming has been measured in various boreholes in North America [2], Russia [3], Northern Europe [4] and China [5]. According to studies at the Qinghai−Tibet Plateau (QTP), surface ground temperatures have increased at an average rate of 0.6 °C per decade during the period from 1980 to 2005 [6]. The continuously rising surface ground temperatures result in significant changes to the permafrost environment [7−8], causing great reductions in the QTP permafrost area [9−11].

Construction of infrastructure in permafrost regions also can induce permafrost environment changes [12]. For highway, embankments constructed above the permafrost inevitably modify the local conditions including micro relief, surface conditions (vegetation and snow covers and water bodies), and physical properties of shallow ground. As a result, imbalance of the surface energy between the atmosphere and the ground occurs, and consequently results in changes of underlying permafrost thermal regime [13]. Due to close relationship between permafrost physical and mechanical properties and its thermal regime, these changes can potentially undermine the long-term stability of highway embankment [14]. The Qinghai−Tibet Highway, of which the construction and reconstruction had lasted about half century, crossed about 750 km of permafrost regions [15]. After upgrading of asphalt pavement in 1973, 60% of the underlying permafrost along the highway had experienced noticeable temperature increase, permafrost table decline, and subsequent talik formation [16−18]. As a consequence, some structural failures of the highway occurred progressively, which

Foundation item: Project(2012CB026106) supported by National Basic Research Program of China; Project(2014BAG05B01) supported by National Key Technology Support Program China; Project(51Y351211) supported by West Light Program for Talent Cultivation of Chinese Academy of Sciences; Project(2013318490010) supported by Ministry of Transport Science and Technology Major Project, China
Received date: 2014−01−08; **Accepted date:** 2014−04−28
Corresponding author: MA Wei, PhD; Tex/fax: +86−931−4967262; E-mail: mawei@lzb.ac.cn

severely lowered service ability of the highway. Among these failures, 83.4% of them were accounted for roadbed thaw settlement induced by underlying permafrost warming and thawing [19−21].

Many researchers studied the embankment stability of Qinghai−Tibet Highway, but these studies were mainly focused on embankment thermal stability, whereas the mechanical and deformation stability of the embankment has received less attention. In this work, the relationships between permafrost degradation and embankment deformation are analyzed based on long-term monitoring data of permafrost temperature and embankment deformation along the Highway. From these analyses, contributions of permafrost warming and degradation to embankment deformation and embankment diseases are discussed. Meanwhile, reliable long-term in-situ monitoring data are provided for future numerical simulation on embankment long-term stability.

2 Data and monitoring methods

2.1 Monitoring site description

The Qinghai−Tibet Highway (QTH) runs approximately 1200 km from Golmud, in the Qinghai province to Lhasa. Approximately 550 km of the QTH runs through the permafrost region. In this work, 8 selected monitoring sites along the QTH reach from Xidatan near the northern permafrost boundary to Anduo at the southern permafrost boundary. Overall, these 8 sites span approximately 3.3 latitude degrees and 2.5 longitude degrees on the eastern Plateau. Elevations of these sites vary from 4516 m at the Xidatan (XT1) site to 5077 m at the Tanggula Mts. (TM1) site, with an average elevation greater than 4700 m. The observation periods at these 8 sites vary from 9 a to 14 a, from 1998 to 2011. Table 1 summarises the geographical locations, altitude, permafrost condition and observation period of these sites.

2.2 Ground temperature monitoring method

Four observation boreholes were established at each site to monitor ground temperature, including natural borehole, roadbed borehole, left road shoulder borehole and right road shoulder borehole (Fig. 1). Ground temperatures from all boreholes were measured at 0.5 to 10 or 15 m. All measurements were taken using a string of thermistors with an increment of 0.5 m in depth. These thermistors were produced by the State Key Laboratory of Frozen Soil Engineering, China. The data were collected twice a month: once at the beginning and once at the middle of each month.

2.3 Embankment deformation monitoring method

Each embankment deformation monitoring site has four transverse sections, and five monitoring points were arranged on each transverse section. Thus, there are a total of 20 deformation-monitoring points at each embankment deformation site (Fig. 2). Serial numbers from 1 to 20 are given to the 20 monitoring points. The monitoring points associated with serial numbers 1, 6, 11 and 16 are located on the right shoulder; serial numbers 2, 7, 12 and 17 are located on the right carriageway; serial numbers 3, 8, 13 and 18 are located in the road centre; serial numbers 4, 9, 14 and 19 are located on the left

Table 1 Geographical data and information of 8 monitoring sites on Qinghai−Tibet Plateau

Site	Area	Location		Altitude/m	Mean annual ground temperature/°C	Observation period
		Latitude	Longitude			
XT1	Xidatan	35°43'05"N	94°04'29"E	4516	−0.51	2003−2011
KL1	Kunlun Mts.	35°39'08"N	94°03'28"E	4724	−2.01	2003−2011
TT1	Tuotuo River	33°52'48"N	92°13'48"E	4572	−0.03	2003−2011
KM1	Kaixin Mts.	33°57'21"N	92°20'23"E	4627	−0.82	2003−2011
TM1	Tanggula Mts.	32°42'30"N	91°52'16"E	4951	−1.20	2003−2011
ZR1	Zhajiazangbu River	32°30'28"N	91°32'03"E	5002	−1.11	1998−2011
TM2	Touerjiu Mts.	32°29'33"N	91°49'17"E	5077	−0.79	1998−2011
NA1	Near Anduo	32°23'00"N	91°42'27"E	4800	−0.16	1998−2011

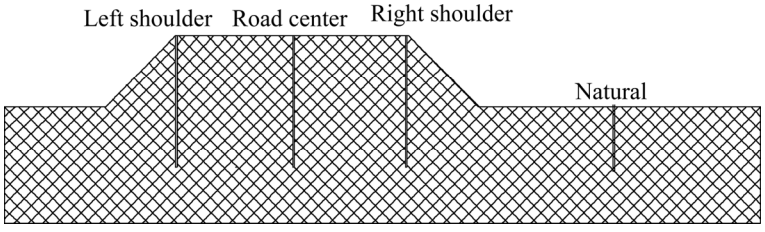

Fig. 1 Boreholes arrangement for ground temperature measurement

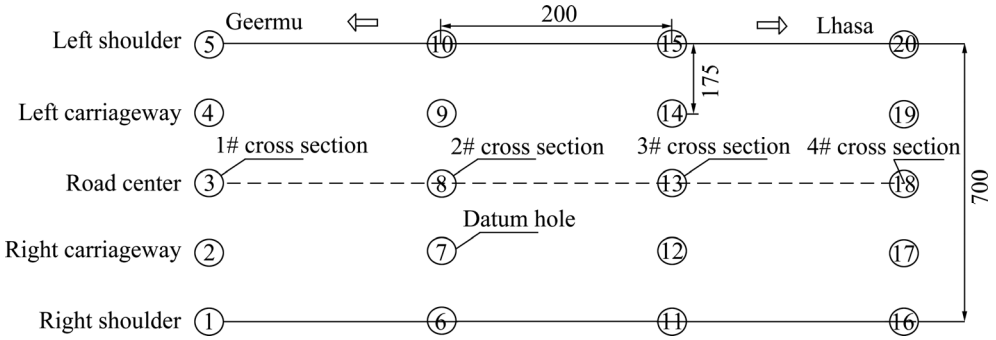

Fig. 2 Measurement point arrangement for embankment deformation monitoring (Unit: cm)

carriageway; serial numbers 5, 10, 15 and 20 are located on the left shoulder. The deformation data are obtained using a surveyor's level and each section has a benchmark installed in the ground with a depth of 16 m.

3 Permafrost warming and degradation beneath asphalt pavement

3.1 Ground temperature beneath asphalt pavement

Based on data for all observation sites, changes in the long-term mean annual soil temperatures under asphalt pavement are different in different permafrost regions. At a depth of 1.0 m, there were strong inter-annual variations in the ground temperatures. These temperatures varied from approximately 1.33 °C at the KL1 site to approximately 4.83 °C at the AD1 site, with an average of 3.12 °C. The average long-term mean annual ground temperature was 0.83 °C at a depth of 5.0 m, varying from −0.85 °C at the KL1 site to approximately 1.64 °C at the AD1 site. The average ground temperature was −0.4 °C at a depth of 10.0 m and the temperatures varied from approximately −1.81 °C at the KL1 site to 0.12 °C at the AD1 site. From this, it can be deduced that the pattern of permafrost temperatures at depths of 5.0 m and 10.0 m are similar to the temperature pattern at depth of 1.0 m (Fig. 3).

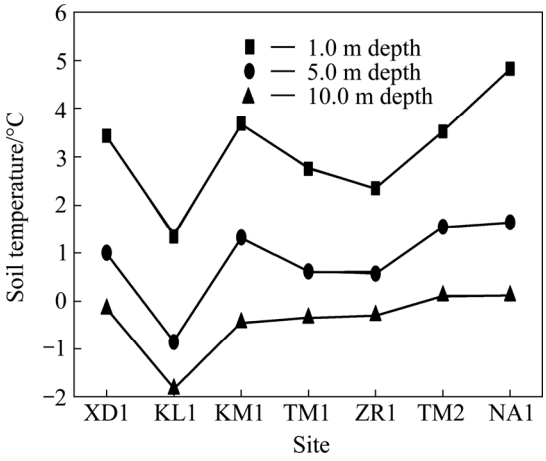

Fig. 3 Long-term mean annual temperatures at different depths under asphalt pavement

3.2 Permafrost table decline beneath asphalt pavement

Continuous ground temperature monitoring data from 8 sites indicated that permafrost table beneath asphalt pavement experienced significant decline during the period from 1998 to 2011 (Fig. 4). During the past 14 a, the permafrost table changes in different permafrost regions have differed greatly. The declining amplitudes of these permafrost tables varied from 0.53 m at the KL1 site to 3.51 m at the NA1 site, with a mean amplitude of 1.65 m. The ALT increases are not only influenced by climate change but also by construction engineering disturbances. Particularly, the strong heat absorbing effect of asphalt pavement further decreases the depth of the permafrost table.

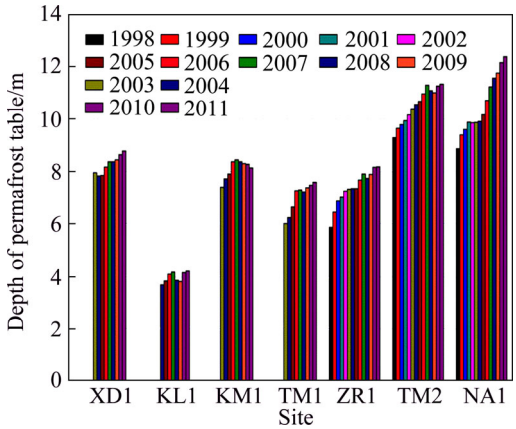

Fig. 4 Changes of permafrost table during monitoring period

3.3 Permafrost temperature increase beneath asphalt pavement

Great heat absorption of asphalt pavement led to an increase in permafrost temperature beneath the embankment. Significant ground temperature changes in the upper permafrost under the asphalt pavement were observed from seven monitoring sites (see Figs. 5 and 6). The permafrost temperature trends over the recorded period for each site are analyzed (Figs. 5(a) and 6(a)), and linear least square correlations were created. An inversely changing trend over the period of records for the embankment was demonstrated (Figs. 5(b) and 6(b)).

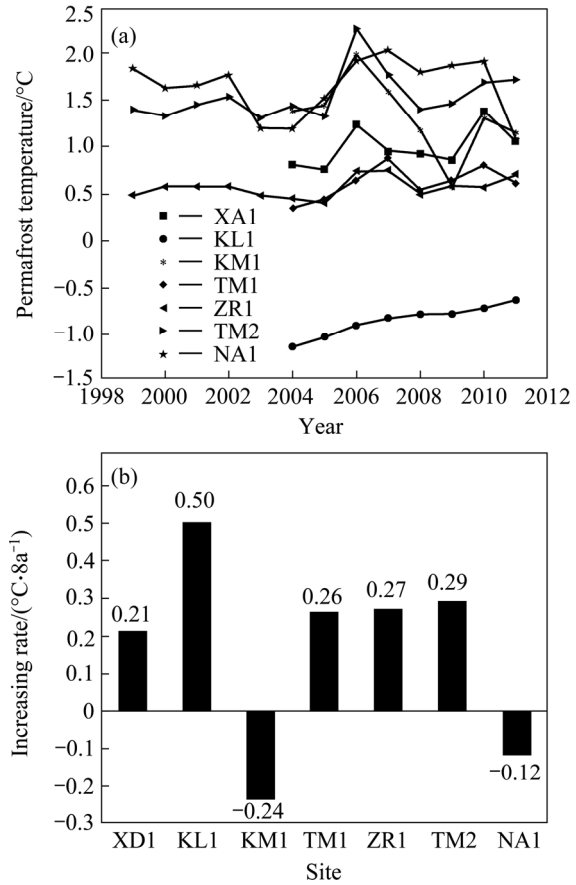

Fig. 5 Mean annual permafrost temperature at 5.0 m beneath embankment (a) and annual increase rate of permafrost temperature (b)

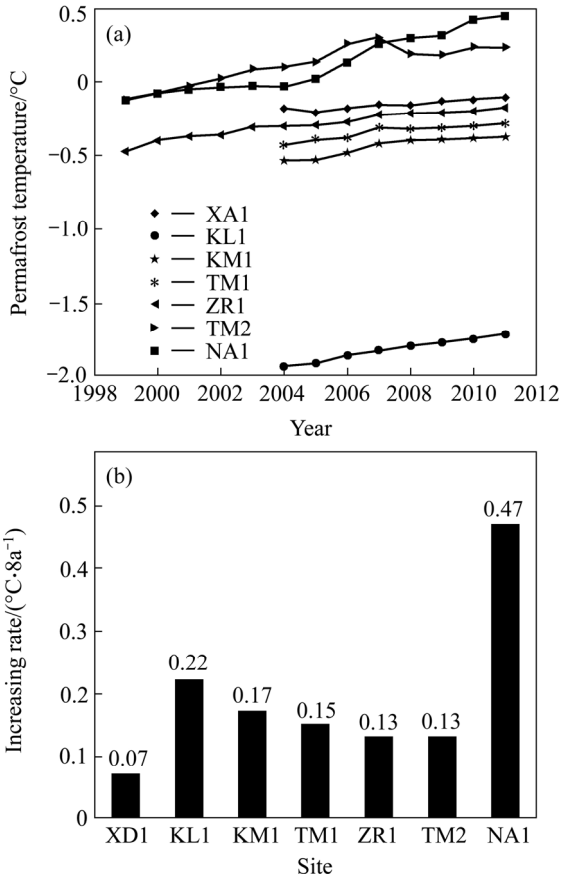

Fig. 6 Mean annual permafrost temperature at 10.0 beneath embankment (a) and annual increase rate of permafrost temperature (b)

At depth of 5.0 m under the asphalt pavement, permafrost temperatures showed a clearly increasing trend at the XD1, KL1, TM1 and TM2 sites (Fig. 5). The increasing rates range from 0.21 °C/8a at the XD1 sites to 0.5 °C/8a at the KL1 sites. The permafrost temperatures show significant decreasing rates at the KM1 and NA1 sites. These rates were −0.24 °C/8a and −0.12 °C/8a, respectively. These decreasing permafrost temperature rates may be the result of an increase of the soil water content, which produces a larger thermal offset and weakens the thermal effect of asphalt pavement [22]. Changes in permafrost temperatures at depth of 10.0 m (Fig. 6) are different from those at depth of 5.0 m (Fig. 5). Permafrost temperatures show a significant increasing trend at all of the observed sites. At depth of 10.0 m below the asphalt pavement, the maximum increasing rate was 0.47 °C/8a at the NA1 site, and the minimum was 0.07 °C/8a at the XD1 site.

4 Characteristics of long-term embankment deformation

4.1 Characteristics of embankment settlement

The stability of the QTH is not only influenced by climate warming, but also by construction engineering disturbation. Based on long-term monitoring data, all embankment deformations at these eight sites mainly perform as settlement deformation and most of the road sections have no obvious frost heave deformation (Fig. 7 and Fig. 8). The QTH embankment settlement has continuously increased in the past nine years and is expected to continue to increase in the future with consideration of permafrost warming and degradation. Embankment deformation can be divided into homogeneous deformation and inhomogeneous deformation based on deformation differences at different embankment areas. In the Tuotuo River area, the settlement value is continuously increasing and the settlement rate is generally consistent at different embankment areas (Fig. 7). The average settlement rate is approximately 4.4 cm/a. This deformation is defined as homogeneous deformation. In the Zhajiazangbu River area, the settlement value is also continuously increasing, but the settlement rate is different (Fig. 8). The maximum settlement rate is 3.1 cm/a and the minimum rate is 1.1 cm/a. This deformation is defined as an inhomogeneous deformation.

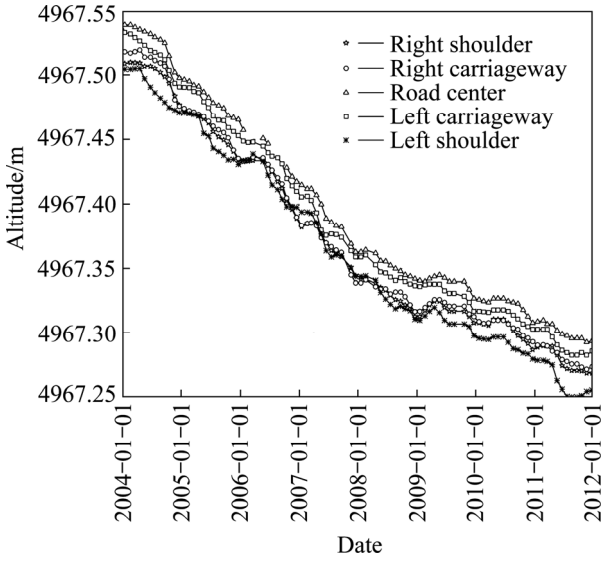

Fig. 7 Long-term deformation of Qinghai−Tibet Highway in Tuotuo River section

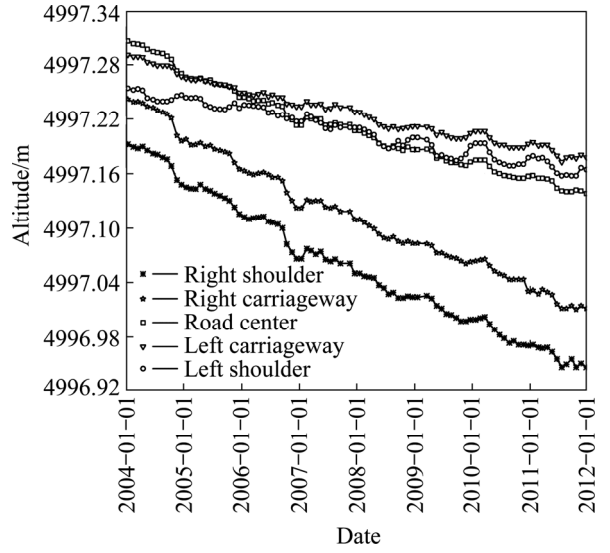

Fig. 8 Long-term deformation of Qinghai−Tibet Highway in Zhajiazangbu River section

There are many reasons for embankment deformation, but temperature changes within underlying permafrost are the main factors. Embankment deformation changes have an even closer relationship with temperature fluctuations on ground surface (Fig. 9 and Fig. 10). Rising temperatures lead to settlement deformation, and the falling temperatures lead to slight frost heave deformation. The embankment deformation process and the changes in temperature are consistent with one another. Thawing settlement deformation is predominant because of the warming and degradation of underlying permafrost.

4.2 Characteristics of longitudinal deformation of embankment

The deformation along the QTX embankment

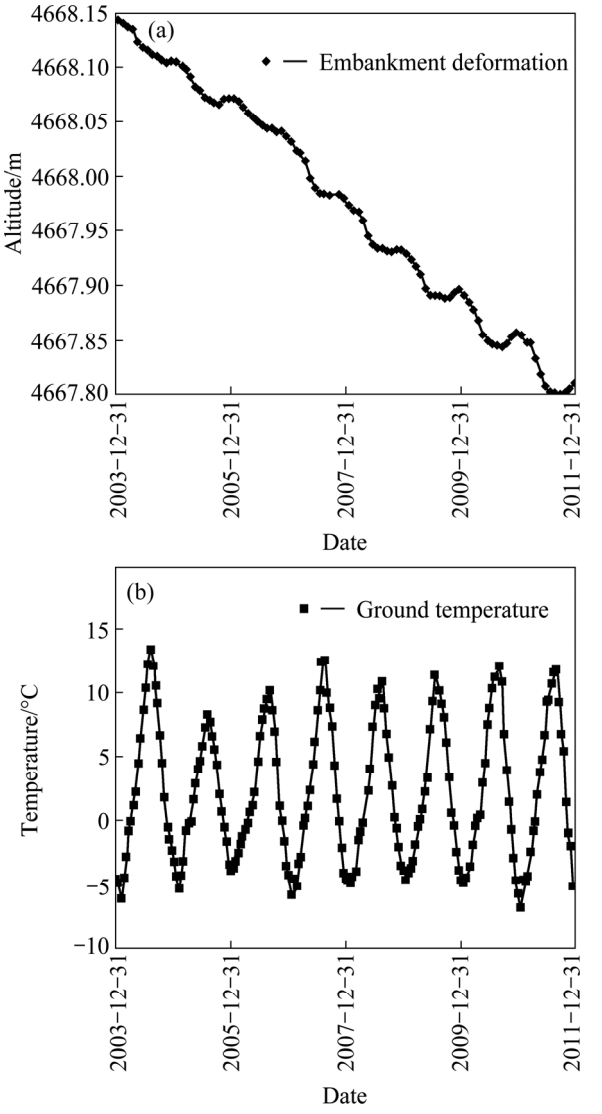

Fig. 9 Relationship between embankment deformation and temperature change in Tuotuo River section

longitudinal causes significant road surface undulation because of the deformation differences at each cross section (Fig. 11). This embankment deformation is defined as longitudinal embankment deformation, and it can be further divided into homogeneous and inhomogeneous deformation according to the settlement difference values on each cross section in the same section of highway. On the XA1, KL1, KM1 and ZR1 highway sections, the settlement values are significantly different from one another and reach 30 cm in some regions, but the maximum and minimum settlement difference values are lower than 5.0 cm. This deformation type is defined as longitudinal homogeneous deformation. On the TT1, TM1, TM2 and NA1 highway sections, the settlement values are larger and meanwhile the differences between the maximum and minimum settlement values are greater than 10.0 cm. For example, the difference values reach up to 20.0 cm at the TT1 site.

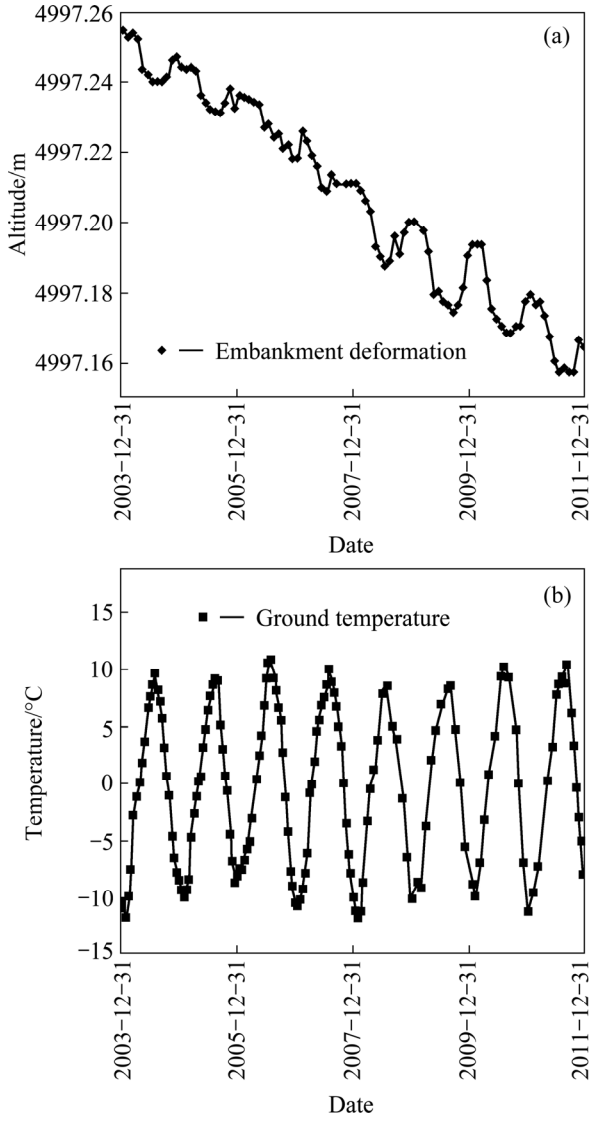

Fig. 10 Relationship between embankment deformation (a) and temperature change (b) in Zhajiazangbu River section

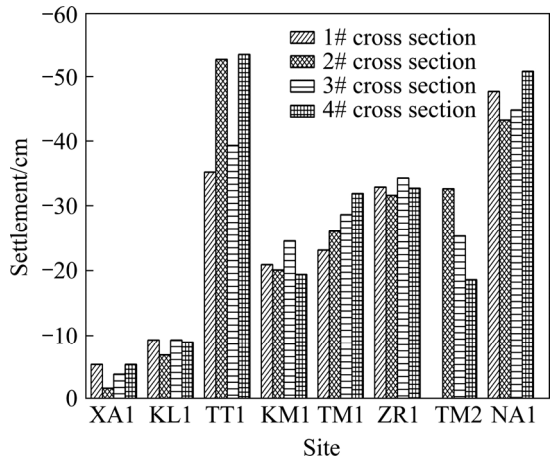

Fig. 11 Longitudinal deformation of Qinghai−Tibet Highway embankment

This deformation is defined as longitudinal inhomogeneous deformation. Longitudinal embankment deformation not only causes highway embankment waves deformation but also has an adverse effect on comfort and driving safety of the road.

4.3 Characteristics of lateral embankment deformation

Because settlements are different in each part of the embankment along the QTX lateral, the embankment tilts towards the side of severe deformation and adversely affects stability. Embankment lateral deformation can also be divided into lateral homogeneous deformation and lateral inhomogeneous deformation. Lateral homogeneous deformation indicates that a smaller deformation difference exists and local subsidence in the embankment is caused. Lateral inhomogeneous deformation brings about longitudinal cracks on embankment surface. At the XA1, KL1, TM1 and TM2 sites, the mean annual deformation difference values are no more than 5.0 cm (Fig. 12). In these areas, lateral homogeneous deformation occurs. It causes the road surface to tilt and creates localised pits. However, the mean annual deformation difference values exceed 10.0 cm, with the maximums up to 20.0 cm at the TT1, KM1, ZR1 and NA1 sites. Lateral inhomogeneous deformations occur in these areas. It causes embankment longitudinal cracks.

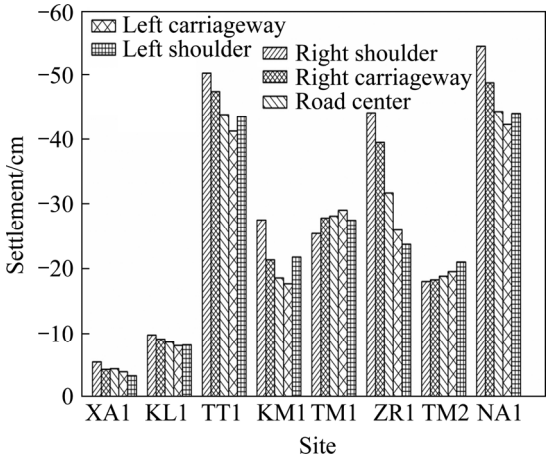

Fig. 12 Lateral deformation of Qinghai−Tibet Highway embankment

5 Discussion and conclusions

Embankment settlements are closely related to permafrost warming and degradation [23]. Generally speaking, thawing settlement of ice-rich permafrost and creep of warming permafrost are main sources of embankment deformation [24]. Embankment deformation can be described by

$$S=Ah_1+\alpha ph_1+\alpha^{\varepsilon}ph_2$$

where S is the total embankment deformation (m); A is

permafrost thawing settlement coefficient; h_1 is the melting layer thickness (m); h_2 is the bearing layer thickness (m); p is the loading intensity (MPa); α is the melting soil compression coefficient (MPa^{-1}); α^{ε} is the permafrost compression coefficient (MPa^{-1}).

According to permafrost degradation processes, embankment settlement generally occurs in the four stages [23]. In the initial permafrost degradation stage (Fig. 13), the embankment settlements occur mainly because of thawing of the upper ice-rich permafrost. During intensive permafrost degradation, the main source of settlements is likely because of permafrost thawing when the MAGT is lower than approximately −1.2 °C (Fig. 13). The embankment begins to settlement at a temperature of approximately −1.2 °C, which is caused by warm permafrost creep. The reasons are that the temperature rise rate and the coefficient of compressibility increase when the permafrost temperature exceeds approximately −1.0 °C [25]. In the vertical talik stage (Fig. 13), both thaw settlement and warm permafrost creep contribute to the total settlement. In the quasi-disappearance stage (not shown in Fig. 13), consolidation of thawed permafrost is the main source of settlement [26]. The QTH has been constructed for nearly 60 a and the permafrost temperatures at the research regions are higher than −1.2 °C (Table 1). Thus, the settlement of the QTH embankment is composed of thawing settlement and warm permafrost creep. Most of the sections of the QTH is in the vertical talik stage.

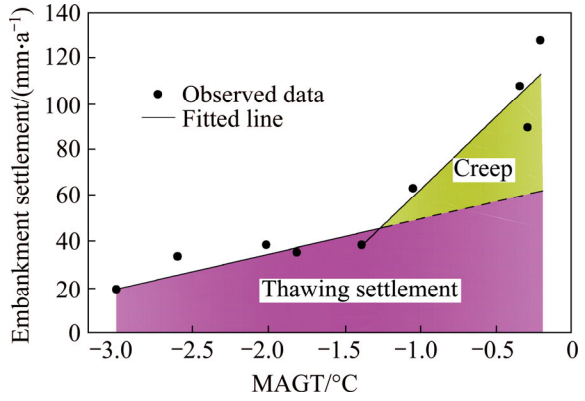

Fig. 13 Mean settlement rates of embankment along QTH from 1998 to 2000 [27]

Because warm permafrost creep is a complicated and long process, its contribution to embankment deformation is difficult to measure. However, the relationships between embankment deformation and permafrost degradation were still determined. Based on the long-term monitoring data (Fig. 14), the rates of permafrost degradation and embankment deformation were differed significantly across different regions. There is also a positive correlation between permafrost degradation and embankment deformation. Greater permafrost degradation rates result in greater embankment deformation, but embankment deformation is caused by many factors, such as, warm permafrost creep, seismic action and vehicle load. It is difficult to use permafrost degradation to explain the causes of embankment deformation. By discussing the contribution of permafrost degradation to embankment deformation, the correlations between permafrost degradation and embankment deformation are analyzed (Fig. 15). The

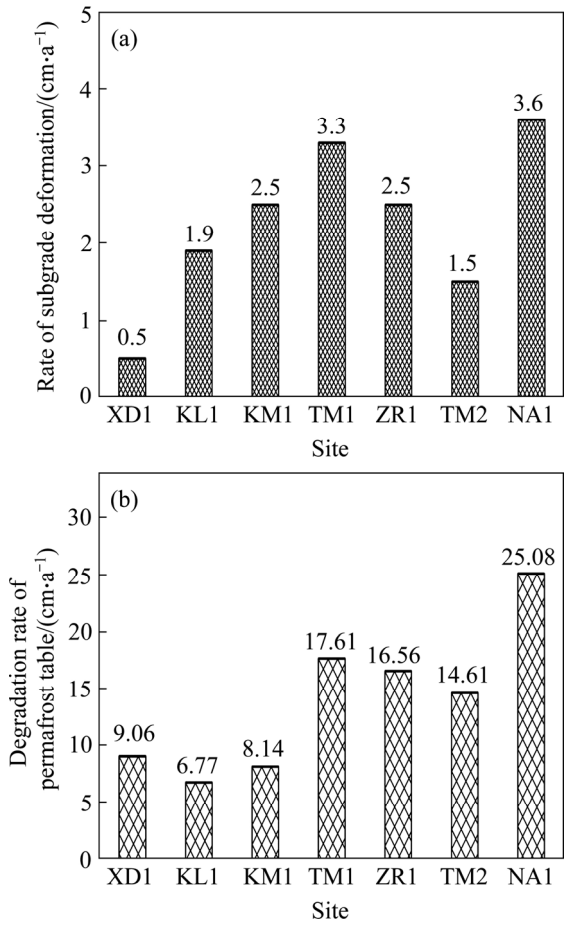

Fig. 14 Relationship between Qinghai−Tibet Highway embankment deformation (a) and permafrost table deformation (b)

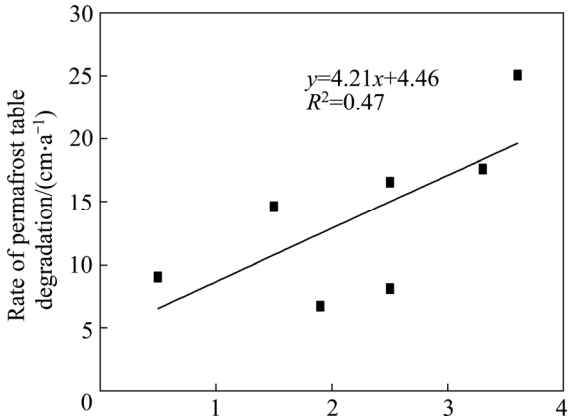

Fig. 15 Relationship between Qinghai−Tibet Highway embankment deformation and permafrost table deformation

regression equation indicates that permafrost degradation and embankment deformation do influence one another.

The results of this work suggest that the main components of embankment deformation are thawing settlement deformation and creep deformation. In other words, the main reasons for embankment deformation are permafrost warming and thawing.

References

[1] ZIMOV S A, SCHUUR E A G, CHAPIN F S. Permafrost and the global carbon budget [J]. Science, 2006, 312: 1612−1613.

[2] SMITH S L, ROMANOVSKY V E, LEWKOWICZ A G, BURN C R, ALLARD M, CLOW G D, YOSHIKAWA K, THROOP J. Thermal state of permafrost in north America: A contribution to the international polar year [J]. Permafrost and Periglacial Processes, 2010, 21(2): 117−135.

[3] ROMANOVSKY V E, DROZDOV D S, OBERMAN N G, MALKOVA G V, KHOLODOV A L, MARCHENKO S S, MOSKALENKO N G, SERGEEV D O, UKRAINTSEVA N G, ABRAMOV A A, GILICHINSKY D A, VASILIEV A A. Thermal state of permafrost in Russia [J]. Permafrost and Periglacial Processes, 2010, 21(2): 136−155.

[4] CHRISTIANSEN H H, ETZELMÜLLER B, ISAKSEN K, JULIUSSEN H, FARBROT H, HUMLUM O, JOHANSSON M, INGEMAN-NIELSEN T, KRISTENSEN L, HJORT J, HOLMLUND P, SANNEL A B K, SIGSGAARD C, ÅKERMAN H J, FOGED N, BLIKRA L H, PERNOSKY M A, ØDEGÅRD R S. Thermal state of permafrost in the Nordic area during the international polar year 2007−2009 [J]. Permafrost and Periglacial Processes, 2010, 21(2): 156−181.

[5] WU Q, ZHANG T, LIU Y. Thermal state of the active layer and permafrost along the Qinghai−Xizang (Tibet) Railway from 2006 to 2010 [J]. The Cryosphere, 2012, 6: 607−612.

[6] XUE Xian, GUO Jian, HAN Bang-shuai, SUN Qing-wei, LIU Li-chao. The effect of climate warming and permafrost thaw on desertification in the Qinghai−Tibet Plateau [J]. Geomorphology, 2009, 108(3/4): 182−190.

[7] OSTERKAMP T E. Characteristics of the recent warming of permafrost in Alaska [J]. Journal of Geophysical Research: Earth Surface, 2007, 112: F02S02, doi:10.1029/2006JF000578.

[8] HARRIS C, MÜHLL D V, ISAKSEN K, HAEBERLI W, SOLLID J L, KING L, HOLMLUND P, DRAMIS F, GUGLIELMIN M, PALACIOS D. Warming permafrost in European mountains [J]. Global Planetary Change, 2003, 39(3/4): 215−225.

[9] CHENG Guo-dong, WU Tong-hua. Responses of permafrost to climate change and their environmental significance, Qinghai−Tibet Plateau [J]. Journal of Geophysical Research, 2007, 112: F02S03. doi: 10.1029/2006 JF000631.

[10] WU Qing-bai, ZHANG Ting-jun. Changes in active layer thickness over the Qinghai−Tibetan Plateau from 1995 to 2007 [J]. Journal of Geophysical Research: Atmospheres, 2010, 115: D09107. doi: 10.1029/2009JD012974.

[11] ZHAO Lin, WU Qing-bai, MARCHENKO S S, SHARKHUU N. Thermal state of permafrost and active layer in central asia during the international polar year [J]. Permafrost and Periglacial Processes, 2010, 21(2): 198−207. doi:10.1002/ppp.688.

[12] LI Jin-peng, SHENG Yu. Analysis of the thermal stability of an embankment under different pavement types in high temperature permafrost regions [J]. Cold Regions Science and Technology, 2008, 54(2): 120−123.

[13] WU Qing-bai, NIU Fu-jun. Permafrost changes and engineering stability in Qinghai−Xizang plateau [J]. Chinese Science Bulletin, 2013, 58(10): 1079−1094. doi:10.1007/s11434-012-5587-z.

[14] ZHENG Bo, ZHANG Jian-ming, QIN Ying-hong. Investigation for the deformation of embankment underlain by warm and ice-rich permafrost [J]. Cold Regions Science and Technology, 2010, 60(2): 161−168.

[15] WU Qing-bai, LIU Yong-zhi, ZHANG Jian-ming, TONG Chang-jiang. A review of recent frozen soil engineering in permafrost regions along Qinghai−Tibet highway, China [J]. Permafrost and Periglacial Processes, 2002, 13: 199−205.

[16] SHENG Yu, ZHANG Jian-ming, LIU Yong-zhi, WU Jing-min. Thermal regime in the embankment of Qinghai−Tibetan Highway in permafrost regions [J]. Cold Region Science and Technology, 2002, 35(1): 35−44.

[17] WANG Shao-ling, MI Hai-zhen. Permafrost change under roadbed after construction of asphalt pavement along with Qing-zang Highway [J]. Journal of Glaciology and Geocryology, 1993, 15(4): 566−573. (in Chinese).

[18] WANG Shao-ling, NIU Fu-jun, ZHAO Lin. Thermal stability of roadbed in permafrost region along the Qinghai−Tibet highway [J]. Cold Regions Science and Technology, 2003, 37(1): 25−34.

[19] LIU Yong-zhi, WU Qing-bai, ZHANG Jian-ming. Deformation of highway roadbed in permafrost regions of the Tibetan Plateau [J]. Journal of Glaciology and Geocryology, 2002, 24(1): 10−15. (in Chinese).

[20] WU Qing-bai, MI Hai-zhen. Predictions and control proposes of frozen ground under asphalt pavement at the high ground temperature section of the Qinghai−Xizang Highway [J]. Hydrogeology and Engineering Geology, 2000, 27(2): 14−17. (in Chinese)

[21] YU Qi-hao, LIU Yong-zhi, TONG Chang-jiang. Analysis of the subgrade deformation of the Qinghai−Tibetan Highway [J]. Journal of Glaciology and Geocryology, 2002, 24(5): 623−627. (in Chinese).

[22] WU Qing-bai, ZHANG Zhong-qiong, LIU Yong-zhi. Long-term thermal effect of asphalt pavement on permafrost under an embankment [J]. Cold Regions Science and Technology, 2010, 60(3): 221−229.

[23] YU Fan, QI Ji-lin, YAO Xiao-liang, LIU Yong-zhi. Degradation process of permafrost underneath embankments along Qinghai−Tibet highway: An engineering view [J]. Cold Regions Sciences and Technology, 2013, 85: 150−156.

[24] MA Wei, LIU Rui, WU Qing-bai. Monitoring and analysis of embankment deformation in permafrost regions of Qinghai−Tibet railway [J]. Rock and Soil Mechanics, 2008, 29: 571−579. (in Chinese)

[25] QI Ji-lin, ZHANG Jian-ming, YAO Xiao-liang, HU Wei, FANG Li-li. Analysis of settlement of constructions in permafrost regions [J]. Rock and Soil Mechanics, 2009, 30(S2): 1−8. (in Chinese)

[26] QI Ji-lin, YAO Xiao-liang, YU Fan, LIU Yong-zhi. Study on thaw consolidation of permafrost under roadway embankment [J]. Cold Regions Science and Technology, 2012, 81: 48−54.

[27] LIU Yong-zhi, WU Qing-bai, ZHANG Jian-ming, SHENG Yu. Deformation of highway roadbed in permafrost regions of Tibetan plateau [J]. Journal of Glaciology and Geocryology, 2002, 24(1): 10−15. (in Chinese)

(Edited by YANG Hua)